IEEE Access
Multidisciplinary | Rapid Review | Open Access Journal

Received June 16, 2018, accepted July 14, 2018, date of publication July 24, 2018, date of current version August 28, 2018.

Digital Object Identifier 10.1109/ACCESS.2018.2859354

Secondary Frequency Regulation Strategy With Fuzzy Logic Method and Self-Adaptive Modification of State of Charge

PEIQIANG LI[1], ZHUANGXI TAN[1], YANJI ZHOU[1], CANBING LI[1,2], (Senior Member, IEEE), RUO LI[1], AND XUEZHONG QI[1]

[1]College of Electrical and Information Engineering, Hunan University, Changsha 410082, China
[2]Hunan Key Laboratory of Intelligent Information Analysis and Integrated Optimization for Energy Internet, Hunan University, Changsha 410082, China

Corresponding author: Canbing Li (lcb@hnu.edu.cn)

This work was supported IN PART by the National Natural Science Foundation of China under Grant 51677059 and in part by the National Key Research Program of China under Grant 2017YFB0902904.

ABSTRACT Battery storage has been adopted to coordinate with generators in automatic generation control (AGC). In this paper, a control strategy of battery storage involved in secondary frequency regulation is proposed. Through the analysis of the control mode based on area control error signal and the control mode based on area regulation requirement signal in AGC, the integrated control strategy was developed, and the switch timing and the output depth of the battery storage were defined. That is, when the system frequency is deteriorated and the frequency deviation $|\Delta f|$ is large, according to the fuzzy logic method, the output power of the battery storage will be smoothened on the basis of the state of charge (SOC). When the system frequency is normal, the frequency deviation $|\Delta f|$ will be small. The remaining frequency regulation capacity of generators can be used to improve the SOC. Furthermore, according to the defined frequency regulation evaluation indexes, MATLAB/Simulink was used to simulate the battery storage coordinating generators for secondary frequency regulation. A typical continuous disturbance was selected in the simulation. The results of the simulation showed that the proposed strategy could enhance the effect of frequency regulation, improve the SOC of the battery storage, and increase the utilization rate of the generator set.

INDEX TERMS Battery storage, secondary frequency regulation, ACE, ARR, fuzzy logic method, SOC.

I. INTRODUCTION

Challenges, such as the shortage of the fossil energy and the problems of environment protection require us to take advantage of renewable energy. With the advantage of abundant reserves and no pollution, renewable energy is expected to ease the fossil energy crisis and the environmental pollution problem considerably [1], and has thus attracted the world's attention.

However, the output of the renewable energy is always random and volatile, and a large-scale input of renewable energy into a power grid will endanger the stability and security of the entire electric power system [2]. Therefore, the methods to maintain a stable power system are worth studying. As the penetration of intermittent renewable generation increases, it is difficult for generators to meet the requirements of grid frequency [3]–[5]. Rapid developments in battery storage technology, however, can provide the new effective means for controlling the frequency quality of the grid connected with the large-scale renewable energy sources [6]–[8].

With respect to the frequency regulation, the characteristics of the battery storage are more suitable in a power system [9], and the battery storage system used here has a faster power regulation speed, which can respond more quickly to the load variation of the system than the generator set. The experimental result in [10] showed that the response speed of the battery storage is 60 times that of thermal power unit. In [11], wind farms and flywheels were introduced to assist the thermal power units in frequency regulation; this significantly reduced the number of actions performed at the thermal power units, relieved the fatigue and wear of the units caused by the frequency regulation, and helped to meet the evaluation index requirements of the frequency regulation.

Secondary frequency regulation requires a higher storage capacity and power than primary frequency regulation.

Thus, it is unrealistic to replace a traditional frequency regulation unit with battery storage [12]; the battery storage can only be used as an auxiliary means to participate in the secondary frequency regulation process with the generator set at present. In most of the earlier studies, the control methods were mainly based on ACE signal and ARR signal. These two ways of control have their own advantages: the former can make full use of the characteristics of the fast response of battery storage, and in the latter case, because of the existence of PI links, the battery can output continuously [13]. A method to combine the advantages of these two control methods and enhance the secondary frequency regulation effect would constitute meaningful research.

On the other hand, in the process of secondary frequency regulation, only if the frequency regulation effect is considered without considering the state of the battery itself, the battery will be damaged. The SOC is closely related to the power output of the battery. With respect to the battery control, the relevant scholars have achieved some results. In [12], a novel algorithm to manage battery charging operations by using a model-based control approach was proposed; the rapid charging strategy was formulated as a linear-time-varying model. Further, for solving the predictive control problem, constraints were imposed to protect the battery from overcharging and overheating. In [13], an advanced machine learning approach for Lithium-Ion battery state estimation was proposed, and a SOC estimator was developed by this learning methodology. In [14], the study focused on the simultaneous optimal component sizing and power management of a fuel cell/battery hybrid bus. All the research achievements reported in the above papers are helpful for considering the battery SOC in the process of secondary frequency regulation.

The main work of this paper is to solve the two problems mentioned above:

(1) Propose a new method to enhance the secondary frequency regulation effect based on ACE signal as well as ARR signal.
(2) On the basis of the enhancement of the effect of frequency regulation, propose a new method to improve the battery state.

In this study, fuzzy control was used to solve the considered problems.

Fuzzy control belongs to the category of intelligent control which has been widely applied in power systems. A fuzzy logic-based controller, in particular, helps in modeling complex system behaviors, where the direct relationship between the system input and the output cannot be expressed through equations, but by utilizing human understanding. In general, a fuzzy controller sets several inputs with only one output. The output value is determined by the input values and the fuzzy control rules. In this study, ACE signal or ARR signal and the SOC of the battery were considered the inputs, and the controller output was the power of the battery storage. When the fuzzy control rules were set appropriately, the regulation effect and the SOC of the battery storage would be enhanced and improved. Therefore, in this study, we utilized fuzzy logic for frequency regulation.

In [15], the study presented a fuzzy logic-based frequency control strategy for distributed PV systems from the viewpoint of the frequency fluctuation problem. Such a fuzzy logic-based frequency controller has three inputs: average insolation, the rate of change of insolation, and the frequency deviation. In [16], the study presented a distributed fuzzy logic controller design for vehicles to grid applications in frequency regulation; the grid was adjusted on the basis of the regulation demand and the SOC of the vehicle battery. In [17], a unique fuzzy logic controller to accurately determine the reference value of active power was devised. All of these studies support the idea of designing a fuzzy controller to smoothen the output power of the battery storage.

This paper can be summarized as follows: first, the two common control modes of the battery storage involved in secondary frequency regulation are analyzed, and the modes are based on ACE signal and ARR signal, respectively. Then, the study combines the advantages of these two modes and uses the fuzzy logic method to smoothen the output power of the battery storage. Lastly, when the system frequency is normal, the remaining frequency regulation capacity of the generators will be used to improve the SOC of the battery. As mentioned, the study establishes an integrated control strategy.

II. CONTROL MODE ANALYSIS

In general, ACE signal is a comprehensive index, mainly used to judge whether the power generation and the load are in a state of equilibrium, which can be calculated by using the grid frequency, the tie-line power flow, and the system electric clock difference.

ACE signal converted by the PI controller, coupled with the secondary frequency regulation dead zone limitation, forms ARR signal. Both the two signals are allocated to the generator sets and the battery storage [18].

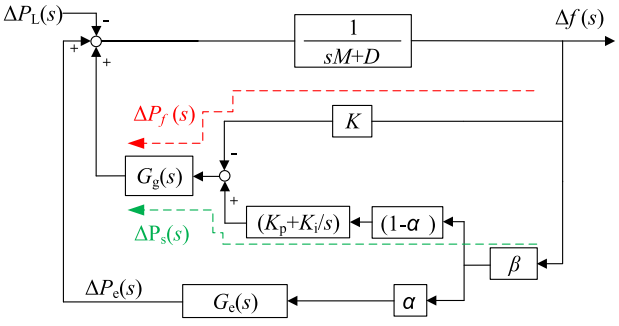

FIGURE 1. Control mode based on ACE signal.

A. CONTROL MODE BASED ON ACE SIGNAL

Fig. 1 presents the dynamic frequency regulation model based on ACE signal.

The battery storage is simplified as transfer function $G_e(s)$, and the generator set is simplified as transfer function $G_g(s)$;

α and $1-\alpha$ are the proportion factors of battery storage and generator set, respectively, involved in secondary frequency regulation. K is the power regulation coefficient of the generator set in the primary frequency regulation, K_p, K_i, and β are the proportional controller coefficient, integral controller coefficient, and frequency deviation coefficient, respectively, of the PI controller. $1/(\mathrm{sM}+\mathrm{D})$ is the transfer function of the interface between the motor and the grid, $\Delta P_\mathrm{L}(\mathrm{s})$ and $\Delta f(\mathrm{s})$ are the load disturbance and the frequency deviation, respectively. Additionally, $\Delta P_f(\mathrm{s})$ and $\Delta P_\mathrm{S}(\mathrm{s})$ are the output depth of the generator set for the primary frequency regulation and for the secondary frequency regulation, respectively, $\Delta P_\mathrm{e}(\mathrm{s})$ is the output depth of the battery storage for the secondary frequency regulation.

The transfer functions of $G_\mathrm{e}(\mathrm{s})$ and $G_\mathrm{g}(\mathrm{s})$ can be expressed as follows:

$$\begin{cases} G_\mathrm{e}(s) = \dfrac{1}{1+sT_\mathrm{e}} \\ G_\mathrm{g}(s) = \dfrac{1+F_\mathrm{HP}T_\mathrm{RH}s}{(1+T_\mathrm{CH}s)(1+T_\mathrm{RH}s)(1+T_g s)}, \end{cases} \tag{1}$$

where T_e is the time constant of the battery storage governor; T_g, T_CH, T_RH, and F_HP are the generator governor constant, steam turbine time constant, reheater time constant, and reheater gain, respectively [19].

The output depth $\Delta P_\mathrm{e}(\mathrm{s})$, $\Delta P_f(\mathrm{s})$ and $\Delta P_\mathrm{S}(\mathrm{s})$ can be calculated on the basis of Fig. 1 as follows:

$$\begin{cases} \Delta P_\mathrm{e}(s) = \beta \cdot \alpha \cdot G_\mathrm{e}(s) \cdot \Delta f(s) \\ \Delta P_f(s) = -K \cdot G_\mathrm{g}(s) \cdot \Delta f(s) \\ \Delta P_\mathrm{s}(s) = \beta \cdot (1-\alpha) \cdot (K_\mathrm{p} + K_\mathrm{i}/s) G_\mathrm{g}(s) \cdot \Delta f(s). \end{cases} \tag{2}$$

The frequency deviation of the system is obtained by combining equations (1) and (2) as follows:

$$\Delta f(\mathrm{s}) = \frac{\Delta P_f(s) + \Delta P_\mathrm{e}(s) + \Delta P_s(s) - \Delta P_L(s)}{sM+D}. \tag{3}$$

The relationship between the system frequency deviation and the load disturbance change rate is obtained by combining equations (2) and (3) as (4), shown at the bottom of this page.

For equation (4), the partial derivative of α is as follows:

$$\frac{\partial \Delta f(s)}{\partial \alpha} = \left(\frac{\Delta f(s)}{\Delta P_L(s)}\right)^2 \cdot \Delta P_L(s) \cdot [\beta \cdot G_\mathrm{e}(s) - G_\mathrm{s}(s)]. \tag{5}$$

The dimensionless sensitivity based on the ACE control mode can be deduced from equation (5):

$$\begin{aligned} S_{\alpha 1} &= \frac{\mathrm{d}\Delta f(s)/\Delta f(s)}{\mathrm{d}\alpha/\alpha} = \frac{\partial \Delta f(s)}{\partial \alpha} \cdot \frac{\alpha}{\Delta f(s)} \\ &= \frac{\alpha \cdot \beta \cdot \Delta f(s)}{\Delta P_L(s)} \left[G_\mathrm{e}(s) - \left(K_\mathrm{p} + \frac{K_\mathrm{i}}{s}\right) G_\mathrm{g}(s) \right]. \end{aligned} \tag{6}$$

According to equation (6), even if a step disturbance occurs, because the frequency deviation and the load increment are always opposite, the first half of the sensitivity expression $a\beta\Delta f(\mathrm{s})/\Delta P_\mathrm{L}(\mathrm{s})$ will be negative. The time constant of $G_\mathrm{e}(\mathrm{s})$ is less than that of $G_\mathrm{g}(\mathrm{s})$, and $S_{\alpha 1}$ is less than zero in the initial stage. Furthermore, the absolute value increases first and then decreases to zero; eventually it goes beyond the zero point until it reaches a steady state. Here, $S_{\alpha 1} = \alpha/(1-\alpha)$, when $S_{\alpha 1}$ is positive; the bigger the value of α is, the higher the frequency deviation will be.

ACE signal does not pass through the PI controller, and the output of the battery storage is directly proportional to the ACE signal. Therefore, this mode can immediately respond to a change in ACE. It is beneficial to recover the deviation of the transient frequency quickly, but doing so will restrain the recovery of the steady-state frequency deviation.

B. CONTROL MODE BASED ON ARR SIGNAL

Fig. 2 presents the dynamic frequency regulation model based on ARR signal.

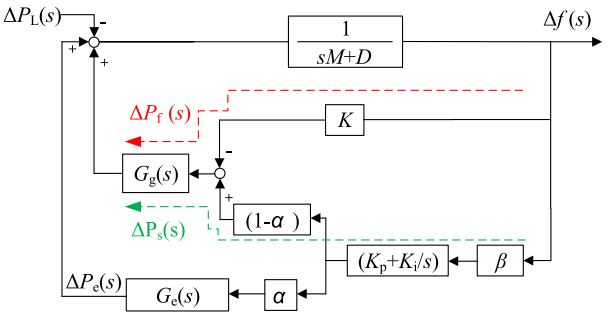

FIGURE 2. Control mode based on ARR signal.

The system parameters will be the same as those in ACE if the control mode is based on ACE. When the dead zone and the limitation are ignored, $\Delta P_f(\mathrm{s})$ and $\Delta P_\mathrm{S}(\mathrm{s})$ will be the output depth of the generator set involved in the primary frequency regulation and the secondary frequency regulation, respectively. $\Delta P_\mathrm{e}(\mathrm{s})$ is the output depth of the battery storage for the secondary frequency regulation. All of these three parameters can be obtained by Fig. 2 as follows:

$$\begin{cases} \Delta P_f(s) = -K \cdot G_g(s) \cdot \Delta f(s) \\ \Delta P_\mathrm{e}(s) = B \cdot \alpha \cdot (K_\mathrm{p} + K_i/s) \cdot G_\mathrm{e}(s) \cdot \Delta f(s) \\ \Delta P_s(s) = B \cdot (1-\alpha) \cdot (K_\mathrm{p} + K_i/s) \cdot G_g(s) \cdot \Delta f(s). \end{cases} \tag{7}$$

According to equations (1) and (7), the frequency deviation of the system is as follows:

$$\Delta f(\mathrm{s}) = \frac{-\Delta P_f(s) + \Delta P_\mathrm{e}(s) + \Delta P_s(s) - \Delta P_L(s)}{sM+D}. \tag{8}$$

$$\frac{\Delta f(\mathrm{s})}{\Delta P_L(\mathrm{s})} = \frac{1}{[-K + \beta \cdot (1-\alpha) \cdot (K_p + K_\mathrm{i}/s)] \cdot G_g(s) + \beta \cdot \alpha \cdot G_\mathrm{e}(s) - (sM+D)}. \tag{4}$$

$$\frac{\Delta f(\mathrm{s})}{\Delta P_L(\mathrm{s})} = \frac{1}{-K \cdot G_g(s) + \beta \cdot (K_p + K_i/s)[(1-\alpha) \cdot G_g(s) + \alpha \cdot G_\mathrm{e}(s)] - (sM+D)}. \tag{9}$$

The relationship between the system frequency deviation and the load disturbance change rate is calculated by combining equations (7) and (8) as (9), shown at the bottom of the previous page.

For equation (9), the partial derivative of the proportional factors of battery storage α can be expressed as follows:

$$\frac{\partial \Delta f(s)}{\partial \alpha} = \left(\frac{\Delta f(s)}{\Delta P_L(s)}\right)^2 \cdot \Delta P_L(s) \cdot \left[\beta\,(K_p + \frac{K_i}{s})G_e(s) - G_s(s)\right]. \tag{10}$$

The dimensionless sensitivity based on the ARR control mode can be deduced from equation (10) as follows:

$$\begin{aligned} S_{\alpha 2} &= \frac{\mathrm{d}\Delta f(s)/\Delta f(s)}{\mathrm{d}\alpha/\alpha} = \frac{\partial \Delta f(s)}{\partial \alpha} \cdot \frac{\alpha}{\Delta f(s)} \\ &= \frac{\alpha \cdot \beta \cdot \left(G_e(s) - G_g(s)\right)}{\Delta P_L(s)}(K_p + \frac{K_i}{s})\Delta f(s). \end{aligned} \tag{11}$$

According to equation (11), the frequency deviation will be increased or decreased by the PI controller and gradually stabilized. Furthermore, the time constant of $G_e(s)$ is less than that of $G_g(s)$, and the frequency deviation and the load increment are always different; therefore, $S_{\alpha 2}$ is always negative in the entire transient process, and the absolute value increases first and then decreases gradually.

ARR signal first goes through the PI link, and the characteristic of its rapid output is partially inhibited. Because of the integral part of the battery storage, the amount of frequency regulation will not be recovered to zero, which can promote the ability of recovering the steady-state frequency deviation.

C. INTEGRATED CONTROL

1. The control mode based on ACE signal makes full use of the fast response characteristic of battery storage and can improve the correction of the transient frequency deviation, whereas the correction of the steady-state frequency deviation is not significant and the mode requires more power reserves.
2. The control mode based on ARR signal can improve the correction of the transient and the steady-state frequency deviation to a certain extent, particularly for the steady-state frequency deviation, but it requires more capacity reserves.

This study maximized the advantages of the ACE control mode to recover the deviation of the transient frequency, as well as the ARR control mode to recover the deviation of the steady-state frequency; an integrated regulation mode of battery storage is presented, as shown in Fig. 3.

III. OUTPUT STRATEGY OF BATTERY

When the frequency of the grid deteriorates, the fuzzy logic method will be introduced to limit the charging power and the discharging power according to the SOC. When the grid frequency is normal, the self-adaptive modification of SOC will be introduced, which implies that the remaining frequency regulation capacity of the generators can be used to improve

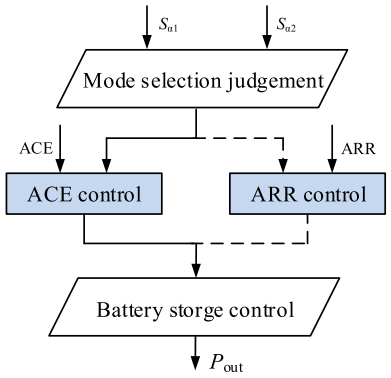

FIGURE 3. Integrated regulation mode of battery storage.

the SOC. Thus, the grid and the status of storage can be mutually perceived.

The discrimination standard for judging the grid status is 30% of the secondary frequency regulation interval [20]. When abs(Δf) $\leq$ 30% $\times$ 0.15 Hz, the self-adaptive modification of SOC should be considered. Fig. 4 shows that how this method make the grid and battery storage interact with each other.

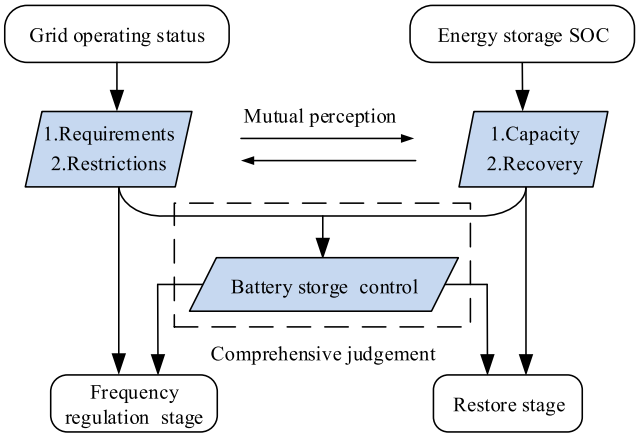

FIGURE 4. Output strategy of battery storage.

A. OUTPUT STRATEGY BASED ON FUZZY LOGIC METHOD

When the system frequency deteriorates, the battery storage will suppress ARR or ACE signal assigned to the storage. On the basis of the fuzzy logic method, the output power takes into account the SOC of the battery storage.

Under normal working conditions, when the SOC value is very low, the discharging power of the battery storage has to be reduced or the charging power has to be increased. Similarly, when the SOC value is very high, the charging power has to be reduced or the discharging power has to be increased. In this study, a fuzzy controller was used to limit the charging and discharging power according to the SOC of the battery storage.

The fuzzy controller designed in this study has two inputs and one output. One input is the ARR or ACE signal, the other

input is the SOC of the battery storage. The output is the smoothened power of the battery storage.

The fuzzy controller adopts a Mamdani-type membership function [21]–[23], and the quantization factors of the input are k_1 and k_2, where k_1 refers to the SOC and k_2 refers to the ARR or ACE signal. The scale factor of the output P_{out} is k_3. These factors can be expressed as shown in (12):

$$\begin{aligned} \mathrm{k}_1 &= 1 \\ \mathrm{k}_2 &= \begin{cases} \dfrac{1}{P_{\text{cm}}} \cdot \eta\%, & P_{\text{int}} < 0 \\ \dfrac{1}{P_{\text{dm}}} \cdot \dfrac{1}{\eta\%}, & P_{\text{int}} > 0, \end{cases} \\ \mathrm{k}_3 &= \begin{cases} P_{\text{cm}} \cdot \eta\%, & P_{\text{int}} < 0 \\ P_{\text{dm}} \cdot \dfrac{1}{\eta\%}, & P_{\text{int}} > 0 \end{cases} \end{aligned} \tag{12}$$

where Pcm and Pdm are the rated charging and discharging power of the battery storage, respectively, $\eta\%$ is the charging or discharging efficiency of the battery storage.

After normalization by the quantization factors, the domains of the inputs of the battery storage are [0, 1] and [−1, 1], as shown in Fig. 5.

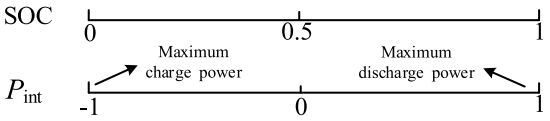

FIGURE 5. Domains of SOC and P_{int}.

The fuzzy sets of the normalized SOC(t) and $\mathrm{P_{int}}$(t) are {NB (Negative Big), NM (Negative Medium), NS (Negative Small), ZO (Almost Zero), PS (Positive Small), PM (Positive Medium), and PB (Positive Big)}. The output P_{out}(t) is decided by the input and the fuzzy logic rule. The domain of the output is [−1, 1], and the fuzzy set of P_{out}(t) includes {NB (Negative Big), NM (Negative Medium), NS (Negative Small), ZO (Almost Zero), PS (Positive Small), PM (Positive Medium), and PB (Positive Big)}. The membership functions of the inputs and the outputs are shown in Figs. 6 and 7. The fuzzy logic rules are presented in Table 1.

TABLE 1. Control rules.

A_{u1} \ A_{u2}	NB	NM	NS	ZO	PS	PM	PB
NB	NB	NM	NS	Z0	Z0	Z0	Z0
NM	NB	NM	NS	Z0	Z0	Z0	Z0
NS	NB	NM	NS	Z0	PS	PM	PB
ZO	NB	NM	NS	Z0	PS	PM	PB
PS	NB	NM	NS	Z0	PS	PM	PB
PM	Z0	Z0	Z0	Z0	PS	PM	PB
PB	Z0	Z0	Z0	Z0	PS	PM	PB

The output of the fuzzy controller is also a fuzzy set, and it can be determined by the centriod method. Furthermore, the modified real-time output power can be expressed as

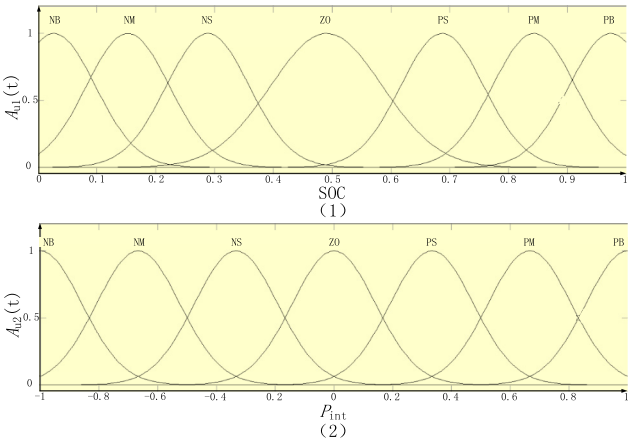

FIGURE 6. Membership function of input.

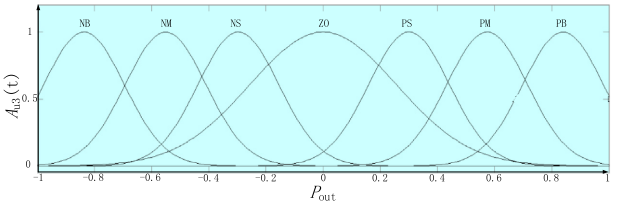

FIGURE 7. Membership function of output.

follows [24]:

$$P_{\text{out}}(\mathrm{t}) = \frac{\int_{u_2}\int_{u_1} A_{u_1}(t) \cdot u_1(t) \cdot A_{u_2}(t) \cdot u_2(t) du_1 du_2}{\int_{u_2}\int_{u_1} A_{u_1}(t) \cdot A_{u_2}(t) du_1 du_2}, \tag{13}$$

where u_1 and u_2 are the quantized SOC(t) and P_{int}(t), respectively, and A_{u1}(t) and A_{u2}(t) are the membership function values of SOC(t) and $\mathrm{P_{int}}$(t), respectively.

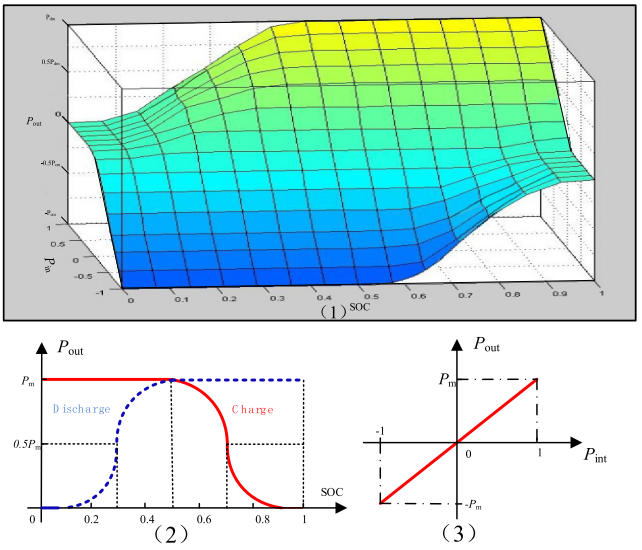

FIGURE 8. Modified real-time output power.

Therefore, the real-time output power P_{out}(t) is obtained as shown in Fig. 8.

The output power of the battery storage is modified by the fuzzy controller. Therefore, the output can be self-adjusted according to the status of the SOC. The method can prevent the battery storage output when the SOC is out of the restriction, which avoid the generation of a secondary disturbance to the power grid and make the grid sense the frequency regulation ability of the battery storage.

B. SELF-ADAPTIVE MODIFICATION OF SOC OF BATTERY STORAGE

When the grid frequency is normal, the remaining frequency regulation capacity of generators can be used to improve the SOC, at this time, the direction of battery output power is opposite to that in the frequency regulation stage. In order to limit the output of the energy storage in the period of self-adaptive modification, the value of SOC is divided into five intervals. These intervals in the ascending order are as follows: $[0, \mathrm{SOC_{min}}]$, $[\mathrm{SOC_{min}}, \mathrm{SOC_{low}}]$, $[\mathrm{SOC_{low}}, \mathrm{SOC_{high}}]$, $[\mathrm{SOC_{high}}\ \mathrm{SOC_{max}}]$, and $[\mathrm{SOC_{max}}, 1]$. The $[\mathrm{SOC_{low}}, \mathrm{SOC_{high}}]$ implies that the SOC values are in the normal interval, and the battery output power is 0.

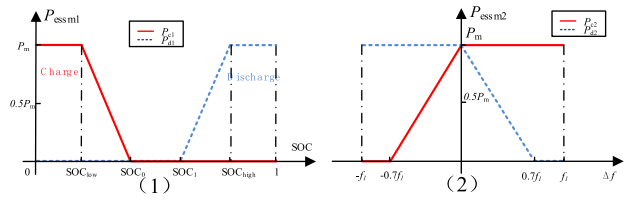

FIGURE 9. Reverse output and restriction.

When the SOC deteriorates ($\Delta f < 0$, SOC $<$ $\mathrm{SOC_{low}}$, or $\Delta f > 0$, SOC $>$ $\mathrm{SOC_{high}}$), and the system is in good condition ($\mathrm{abs}(\Delta f) \le f_1$ Hz, $f_1 = 30\% \times 0.15$ Hz), the battery begins to output. At the same time, the output of the battery storage should be ensured that the frequency deviation don't increase beyond the normal regulatory region ($\mathrm{abs}(\Delta f) \ge f_1$ Hz, $f_1 = 30\% \times 0.15$ Hz). The battery output power is as shown in Fig. 9. (1) and equations (14). The output restriction is shown in Fig. 9. (2) and equations (15).

$$P_{c1} = \begin{cases} P_m & SOC \le SOC_{\mathrm{low}} \\ P_m \cdot (2 - SOC/0.2) & SOC_{\mathrm{low}} < SOC \le SOC_0 \\ 0 & SOC > SOC_0 \end{cases}$$

$$P_{d1} = \begin{cases} 0 & SOC \le SOC_1 \\ P_m \cdot (5 \cdot SOC - 3) & SOC_1 < SOC \le SOC_{\mathrm{high}} \\ P_m & SOC > SOC_{\mathrm{high}} \end{cases} \quad (14)$$

WhereP_{c1} is the charging power of the battery storage; P_{d1} is the discharging power of the battery storage; P_m is the rated power of the battery storage.

$$P_{c2} = \begin{cases} 0 & \Delta f \le -0.7 f_1 \\ P_m(1 + \Delta f / 0.7 f_1) & -0.7 f_1 < \Delta f \le 0 \\ P_m & \Delta f > 0 \end{cases}$$

$$P_{d2} = \begin{cases} P_m & \Delta f \le 0 \\ P_m(1 - \Delta f / 0.7 f_1) & 0 < \Delta f \le 0.7 f \\ 0 & \Delta f > 0.7 f \end{cases} \quad (15)$$

where P_{c2} and P_{d2} are the charging and discharging restrictions, respectively, which ensure that the frequency deviation does not cross the normal regulation area. Furthermore, f_1 refers to the size of the adjustment interval, as shown in Fig. 9(2).

When the SOC of the battery storage deteriorates and the system is in good condition, the storage output for the SOC modification appears as shown in Fig. 10.

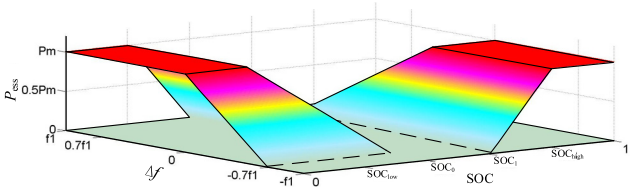

FIGURE 10. Battery storage output in self-adaptive modification of SOC.

The battery storage output power P_{ess} in self-adaptive modification stage can be expressed as follows:

$$P_{\mathrm{ess}} = \begin{cases} -\min\{|P_{c1}|, |P_{c2}|\}, & SOC < SOC_{\mathrm{low}} \\ \min\{|P_{d1}|, |P_{d2}|\}, & SOC > SOC_{\mathrm{high}} \end{cases} \quad (16)$$

The strategy of the self-adaptive modification of SOC enables the battery storage to sense the grid status. When the grid frequency is normal and the SOC deteriorates, the battery performs a self-adaptive modification to improve the SOC. Therefore, the battery storage can provide a higher frequency regulation capacity for the subsequent tasks.

IV. INTEGRATED CONTROL STRATEGY

The integrated control strategy is involved in the secondary frequency regulation stage, and it is necessary to confirm the switching timing of the battery storage. Furthermore, the fuzzy logic method and the SOC self-adaptive modification are combined to determine the battery output depth. In this study, the evaluation indexes are also defined.

A. SWITCHING TIMING OF THE BATTERY STORAGE

The amount of the ACE signal is obviously higher than that of the ARR signal in the transient state, whereas in the steady state, the battery storage based on the ACE signal gradually reduces the output. The storage based on the ARR signal continues to provide the same output because of the integral link, which is favorable for reducing the steady-state frequency deviation. In this section, the battery storage control mode and the switching timing are as follows:

1. *Start moment:* As the ACE signal exceeds the limit set by the dead zone, the battery storage will begin to participate in the secondary frequency regulation.
2. *Switching timing:* According to the system status, the sensitivities of the ACE signal $S_{\alpha 1}$ and the ARR signal $S_{\alpha 2}$ are calculated and the control mode is selected.

3. *Exit timing:* As the ACE signal or the ARR signal falls back into the dead zone; the battery storage will stop the output.

B. INTEGRATED CONTROL STRATEGY FLOW

On the basis of the previous analysis, the fuzzy logic method and the SOC self-adaptive modification strategy are combined. The concrete steps of the battery storage involved in the secondary frequency regulation are as follows:

1. Determine whether the battery storage is involved in the secondary frequency regulation according to the set value of the dead zone.
2. After the battery storage participates in the secondary frequency regulation, adopt the ACE control mode. Then, obtain the ARR signal, and calculate the real-time sensitivity of ACE signal S α 1 and ARR signal S α 2. When $S_{\alpha1}/\Delta f > S_{\alpha2}/\Delta f$, select the ACE control mode. When $S_{\alpha1}/\Delta f < S_{\alpha2}/\Delta f$, switch to the ARR control mode. The control mode and the switching timing of the battery storage are obtained.
3. According to the system frequency deviation Δf and the SOC of the battery, judge the status of the battery storage and the system. When the system is in good condition but the SOC is poor, the SOC can be modified by the remaining frequency regulation capacity of the generator set; otherwise, the battery output is based on the fuzzy logic method.
4. Finally, determine whether the ACE signal or the ARR signal falls back into the dead zone, and determine the exit timing of the battery.

The integrated control strategy flow is as shown in Fig. 11.

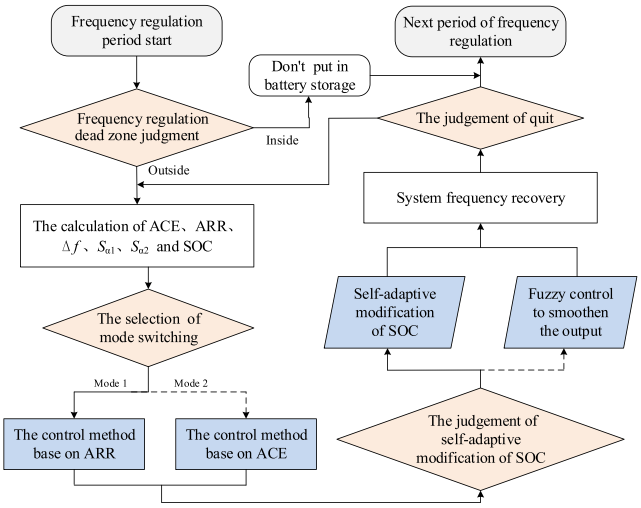

FIGURE 11. Integrated control strategy flowchart.

C. EVALUATION INDEX

The evaluation indexes of the frequency regulation are related to the frequency regulation power supply, defined as follows [25], [26].

1) EVALUATION INDEXES OF FREQUENCY EFFECT

Δf_0, Δf_m, Δf_s, t_0, t_m, and t_s are the initial frequency deviation, the maximum frequency deviation, the steady-state frequency deviation, and their respective moments. Δf_{rms} is the root mean square value of frequency deviation Δf, V_m is the frequency slip rate, $V_m = (\Delta f_0 - \Delta f_m)/(t_m - t_0)$, and V_r is the frequency reset rate, $V_r = (\Delta f_s - \Delta f_m)/(t_s - t_m)$. The definition shows that both the smaller V_m and the faster the V_r can contribute to a better frequency regulation effect.

2) CONTRIBUTION INDEXES OF POWER SUPPLY

SOC_{rmse} is the root mean square error of the SOC and its reference value (0.5 in this study); the smaller the value of SOC_{rmse} is, the closer the value of the SOC will be to 0.5, that is, the energy storage can maintain a better SOC. W_{ess} is the total contribution energy of the battery storage to the secondary frequency regulation, and W_{gen} is the total contribution energy of the generator set to the secondary frequency regulation. Both W_{ess} and W_{gen} can be integrated and calculated during the t_0–t_s period. The definition shows that the greater the value of W_{ess} or W_{gen} is, the greater the contribution of power supply to the secondary frequency regulation will be.

TABLE 2. Model parameters.

Parameter	Value	Parameter	Value
Power reference (MW)	1000	Climbing speed (MW/min)	30
Reserve capacity (MW)	±60	Frequency reference (Hz)	50
Energy storage capacity (MWh)	2.5	Storage power (MW)	15
M (p.u.)	10	D (p.u.)	1
K (p.u.)	20	B (p.u.)	21
T_g (s)	0.08	K_p (p.u)	-0.822
a	0.2	K_i (p.u)	-0.16
T_{CH}、T_{RH} (s)	0.3、10	F_{HP} (p.u.)	0.5

V. SIMULATION AND VERIFICATION

A. SIMULATION PARAMETERS

The typical single-area system model was adopted in this study and the fixed frequency control (FFC) method was used to make the battery storage coordinates of the grid participate in the secondary frequency regulation [27], [28]. The parameter settings of the simulation system are given in Tables 2 and 3.

B. SIMULATION RESULTS ANALYSIS

The control mode based on the ARR signal is called "ARR control", and the control mode based on the ACE signal is called "ACE control". The integrated control mode presented in this paper is called "Integrated control". The control mode without battery storage is called "No battery storage".

The typical continuous load disturbance condition of 120-min in the region of Chenzhou, Hunan, China

TABLE 3. Relevant parameters.

Parameter	Value	Parameter	Value	Parameter	Value
SOC_{min}	0.1	SOC_{low}	0.2	SOC_0	0.4
SOC_{max}	0.9	SOC_{high}	0.8	SOC_1	0.6
f_l(Hz)	0.045	ACE_{dead}	1.05	ARR_{dead}	1.05

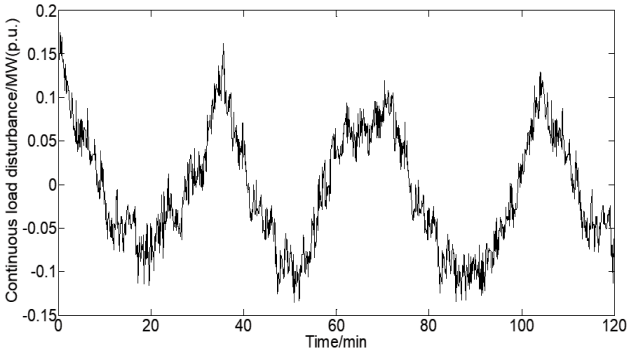

FIGURE 12. 120-min continuous load disturbance.

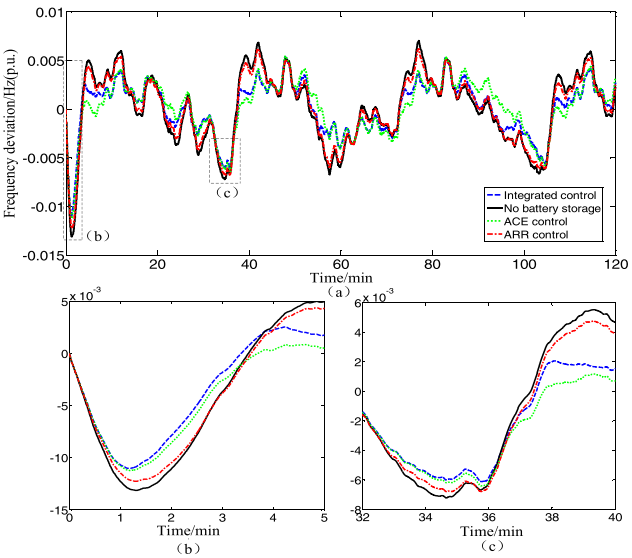

FIGURE 13. System frequency deviation.

in 2014 was selected, as shown in Fig. 12. For the different control modes, the frequency deviation of the system is shown in Fig. 13. Fig. 14 shows the power supply contribution of the generator set and the battery. Fig 15 (a), 15 (b) and 15(c) respectively describe the effect of using three control strategies when the initial SOC of the battery is 0.3, 0.5, and 0.8. Fig 15(d) describes the difference in the control effects in different SOC initial values using the integrated control strategy of this paper. The frequency regulation effect and power supply contribution indexes are shown in Table 4-6.

From Fig. 12 to Fig. 15, Table 4-6, the following conclusions were drawn from three aspects:

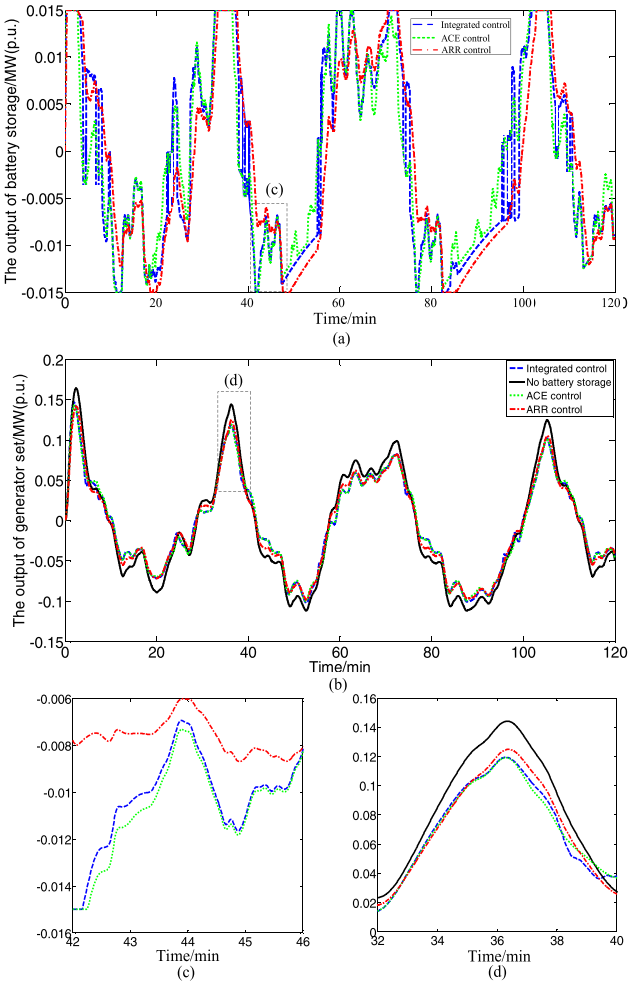

FIGURE 14. Power supply contribution.

1) FREQUENCY REGULATION EFFECT

As shown in Fig. 13 and Table 4-6, when the battery storage with different initial values of SOC is involved in the frequency regulation, the maximum frequency deviation Δf_m and the frequency slip rate V_m decrease while the frequency reset rate V_r increase, according to the previous evaluation indexes. The participation of energy storage can improve the effect of frequency regulation.

"ACE control" is essentially a proportional derivative (PD) control mode, which can improve the correction of the transient frequency deviation, whereas the correction of the steady-state frequency deviation is suppressed. "ARR control" is essentially a proportional integral (PI) control mode, that is, in this mode, continuous output is beneficial to restore the steady-state frequency deviation, but it has little effect on the frequency improvement of the system under a large frequency disturbance.

The calculation results can also be obtained from Table 4-6. The average frequency slip rate V_m of "integrated control" with the three sets of data is 1.06% and 1.28% lower than that in the ACE and ARR control mode, respectively. The average frequency reset rate V_r of "integrated control" with

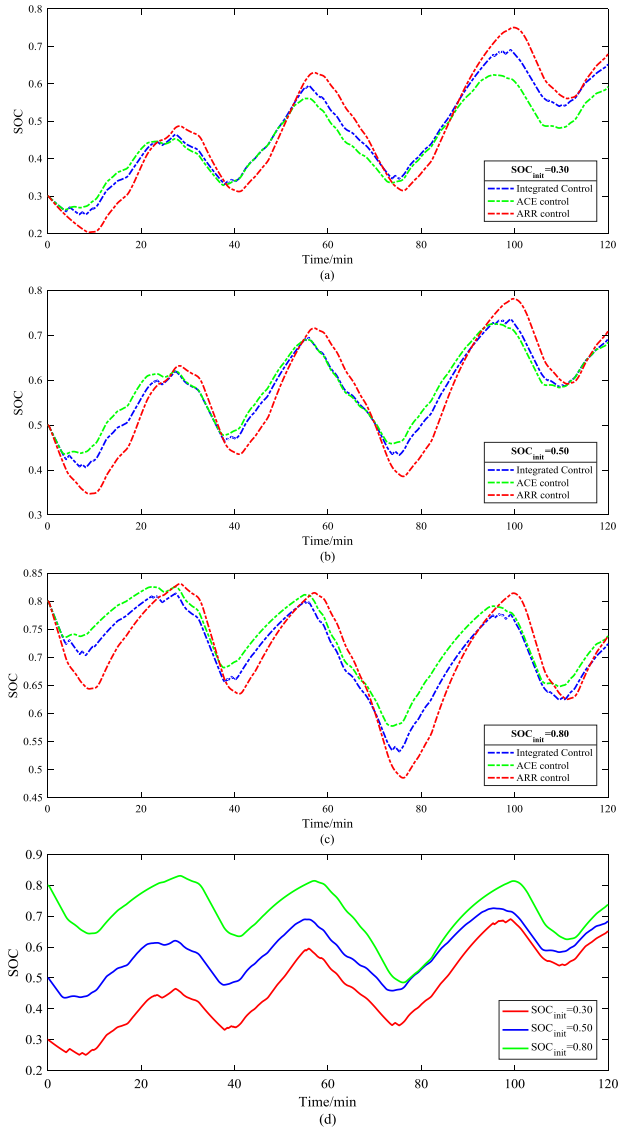

FIGURE 15. SOC of battery storage.

TABLE 4. The frequency regulation effect and power supply contribution indexes when the initial SOC is 0.3.

Evaluation index	Integrated control	No battery storage	ACE control	ARR control
$\lvert\Delta f_m\%\rvert$	0.01158	0.01379	0.01210	0.01364
V_m	0.00768	0.00825	0.00776	0.00775
V_r	1.921×10^{-3}	1.006×10^{-3}	1.362×10^{-3}	1.876×10^{-3}
W_{gen}	0.0978	0.1152	0.0964	0.0952
W_{ess}	0.0187	–	0.0155	0.0244
SOC_{rmse}	0.1240	–	0.1119	0.1524

the three sets of data is 29.42% and 5.55% higher than that in the ACE and ARR control mode, respectively. The integrated control mode has better frequency regulation effect than ACE control mode and ARR control mode.

TABLE 5. The frequency regulation effect and power supply contribution indexes when the initial SOC is 0.5.

Evaluation index	Integrated control	No battery storage	ACE control	ARR control
$\lvert\Delta f_m\%\rvert$	0.01117	0.01379	0.01152	0.01299
V_m	0.00740	0.00826	0.00748	0.00751
V_r	1.520×10^{-3}	1.006×10^{-3}	1.235×10^{-3}	1.431×10^{-3}
W_{gen}	0.0977	0.1152	0.0964	0.0952
W_{ess}	0.0186	–	0.0155	0.0246
SOC_{rmse}	0.1130	–	0.1134	0.1333

TABLE 6. The frequency regulation effect and power supply contribution indexes when the initial SOC is 0.8.

Evaluation index	Integrated control	No battery storage	ACE control	ARR control
$\lvert\Delta f_m\%\rvert$	0.01117	0.01379	0.01152	0.01299
V_m	0.00740	0.00826	0.00748	0.00751
V_r	1.466×10^{-3}	1.006×10^{-3}	1.181×10^{-3}	1.357×10^{-3}
W_{gen}	0. 1001	0.1152	0.0990	0.0982
W_{ess}	0.0159	–	0.0128	0.0212
SOC_{rmse}	0.2210	–	0.2403	0.2217

2) POWER SUPPLY CONTRIBUTION

From Fig. 14 and Table 4-6, the average contribution of generator set of "Integrated control" with the three sets of data is 1.30% and 2.43% higher than that in the ACE and ARR control mode, respectively, which implies that the proposed method improves the utilization rate of the generator set.

As far as the battery storage contribution is concerned, the contribution of "Integrated control" is between that of "ACE control" and that of "ARR control". However, the ACE control method is at the expense of a certain frequency regulation effect. It shows that the proposed method can reduce the capacity requirement of the battery storage to a certain extent.

3) IMPROVEMENT OF BATTERY STORAGE SOC

The SOC should always be around 50% to provide the maximal flexibility, i.e. the smaller the value of SOC_{rmse} is, the closer the change of the SOC will be to 0.5. Although the SOC_{rmse} in "ACE control" is smaller than that in the integrated control mode in Fig. 15 (a) and Table 4, the SOC_{rmse} in "Integrated control" is smaller than that in the ACE control and ARR control mode in other conditions in Fig. 15 and Table 4-6. Moreover, the average value of SOC_{rmse} in "Integrated control" with the three sets of data is minimum, which implies that the proposed method can maintain the best battery state and can prevent battery overcharge or overdischarge. Fig. 15 (d) shows the change process of SOC when taking different initial values of SOC in "Integrated control", the change trends of the SOC are the same implying the rationality and effectiveness of "Integrated control".

VI. CONCLUSION

An integrated control mode based on the fuzzy logic method and the self-adaptive modification of SOC was proposed in this study. The characteristics of the ACE control mode and the ARR control mode were analyzed. Further, the integrated control mode combines the advantages of the two modes. The simulation verification shows that the control strategy proposed in this paper can recover the deviation of the transient frequency quickly, as well as promote the ability of recovering the steady-state frequency deviation. In contrast, the utilization rate of the generator set can be improved, and the state of the battery storage can be better.

REFERENCES

[1] X. Hu, Y. Zou, and Y. Yang, "Greener plug-in hybrid electric vehicles incorporating renewable energy and rapid system optimization," *Energy*, vol. 111, pp. 971–980, Sep. 2016.
[2] S. Saxena and Y. V. Hote, "Load frequency control in power systems via internal model control scheme and model-order reduction," *IEEE Trans. Power Syst.*, vol. 28, no. 3, pp. 2749–2757, Aug. 2013.
[3] Y. Guo, D. Zhang, J. Wan, and D. Yu, "Influence of direct air-cooled units on primary frequency regulation in power systems," *IET Gener. Transmiss. Distrib.*, vol. 11, no. 17, pp. 4365–4372, 2017.
[4] F. Yang, J. He, and D. Wang, "New stability criteria of delayed load frequency control systems via infinite-series-based inequality," *IEEE Trans. Ind. Informat.*, vol. 14, no. 1, pp. 231–240, Jan. 2018.
[5] D. Ochoa and S. Martinez, "Fast-frequency response provided by DFIG-wind turbines and its impact on the grid," *IEEE Trans. Power Syst.*, vol. 32, no. 5, pp. 4002–4011, Sep. 2017.
[6] Y. Yang, Q. Ye, L. J. Tung, M. Greenleaf, and H. Li, "Integrated size and energy management design of battery storage to enhance grid integration of large-scale PV power plants," *IEEE Trans. Ind. Electron.*, vol. 65, no. 1, pp. 394–402, Jan. 2018.
[7] A. Papavasiliou and S. S. Oren, "Large-scale integration of deferrable demand and renewable energy sources," *IEEE Trans. Power Syst.*, vol. 29, no. 1, pp. 489–499, Jan. 2014.
[8] W. Chen, X. Wu, L. Yao, W. Jiang, and R. Hu, "A step-up resonant converter for grid-connected renewable energy sources," *IEEE Trans. Power Electron.*, vol. 30, no. 6, pp. 3017–3029, Jun. 2015.
[9] H. Bevrani, A. Ghosh, and G. Ledwich, "Renewable energy sources and frequency regulation: Survey and new perspectives," *IET Renew. Power Gener.*, vol. 4, no. 5, pp. 438–457, 2010.
[10] F. Zhang, Z. Hu, X. Xie, J. Zhang, and Y. Song, "Assessment of the effectiveness of energy storage resources in the frequency regulation of a single-area power system," *IEEE Trans. Power Syst.*, vol. 32, no. 5, pp. 3373–3380, Sep. 2017.
[11] A. A. Thatte, F. Zhang, and L. Xie, "Coordination of wind farms and flywheels for energy balancing and frequency regulation," in *Proc. IEEE Power Energy Soc. General Meeting*, Jul. 2011, pp. 1–7.
[12] H. Yang, S. Li, Q. Li, and W. Chen, "Hierarchical distributed control for decentralized battery energy storage system based on consensus algorithm with pinning node," *Protection Control Mod. Power Syst.*, vol. 3, no. 1, p. 6, 2018.
[13] R. G. de Almeida and J. A. P. Lopes, "Participation of doubly fed induction wind generators in system frequency regulation," *IEEE Trans. Power Syst.*, vol. 22, no. 3, pp. 944–950, Aug. 2007.
[14] X. Hu, S. E. Li, and Y. Yang, "Advanced machine learning approach for lithium-ion battery state estimation in electric vehicles," *IEEE Trans. Transport. Electrific.*, vol. 2, no. 2, pp. 140–149, Jun. 2016.
[15] X. Hu, N. Murgovski, L. M. Johannesson, and B. Egardt, "Optimal dimensioning and power management of a fuel cell/battery hybrid bus via convex programming," *IEEE/ASME Trans. Mechatronics*, vol. 20, no. 1, pp. 457–468, Feb. 2015.
[16] M. Datta and T. Senjyu, "Fuzzy control of distributed PV inverters/energy storage systems/electric vehicles for frequency regulation in a large power system," *IEEE Trans. Smart Grid*, vol. 4, no. 1, pp. 479–488, Mar. 2013.
[17] G. Li, J. Wu, J. Li, T. Ye, and R. Morello, "Battery status sensing software-defined multicast for V2G regulation in smart grid," *IEEE Sensors J.*, vol. 17, no. 23, pp. 7838–7848, Dec. 2017.
[18] S. Zhang, Y. Mishra, and M. Shahidehpour, "Fuzzy-logic based frequency controller for wind farms augmented with energy storage systems," *IEEE Trans. Power Syst.*, vol. 31, no. 2, pp. 1595–1603, Mar. 2016.
[19] M. R. A. Paternina, J. M. Ramirez-Arredondo, J. D. Lara-Jiménez, and A. Zamora-Mendez, "Dynamic equivalents by modal decomposition of tie-line active power flows," *IEEE Trans. Power Syst.*, vol. 32, no. 2, pp. 1304–1314, Mar. 2017.
[20] P. Fortenbacher, J. L. Mathieu, and G. Andersson, "Modeling and optimal operation of distributed battery storage in low voltage grids," *IEEE Trans. Power Syst.*, vol. 32, no. 6, pp. 4340–4350, Nov. 2017.
[21] A. Delavari and I. Kamwa, "Improved optimal decentralized load modulation for power system primary frequency regulation," *IEEE Trans. Power Syst.*, vol. 33, no. 1, pp. 1013–1025, Jan. 2018.
[22] L. P. Perera, J. P. Carvalho, and C. G. Soares, "Solutions to the failures and limitations of mamdani fuzzy inference in ship navigation," *IEEE Trans. Veh. Technol.*, vol. 63, no. 4, pp. 1539–1554, May 2014.
[23] S. Galichet and L. Foulloy, "Fuzzy controllers: Synthesis and equivalences," *IEEE Trans. Fuzzy Syst.*, vol. 3, no. 2, pp. 140–148, May 1995.
[24] S. Halgamuge, "A trainable transparent universal approximator for defuzzification in Mamdani-type neuro-fuzzy controllers," *IEEE Trans. Fuzzy Syst.*, vol. 6, no. 2, pp. 304–314, May 1998.
[25] J. Yu, J. Liu, Z. Wu, and H. Fang, "Depth control of a bioinspired robotic Dolphin based on sliding-mode fuzzy control method," *IEEE Trans. Ind. Electron.*, vol. 65, no. 3, pp. 2429–2438, Mar. 2018.
[26] L. Wei, Y. Li, Y. Chi, and Y. Su, "Study on characteristics evaluation index of renewable power output and application on renewable energy development planning," in *Proc. Int. Conf. Renew. Power Gener. (RPG)*, Beijing, China, 2015, pp. 1–6.
[27] E. Pyetan and S. Akselrod, "Do the high-frequency indexes of HRV provide a faithful assessment of cardiac vagal tone? A critical theoretical evaluation," *IEEE Trans. Biomed. Eng.*, vol. 50, no. 6, pp. 777–783, Jun. 2003.
[28] R. de Jesus Romero-Troncoso, "Multirate signal processing to improve FFT-based analysis for detecting faults in induction motors," *IEEE Trans Ind. Informat.*, vol. 13, no. 3, pp. 1291–1300, Jun. 2017.

PEIQIANG LI was born in Xinzhou, Shanxi, China, in 1975. He received the B.S. degree in electrical engineering from Changsha Electric Power University, Changsha, China, in 1997, the master's and Ph.D. degrees in electrical engineering from Hunan University in 2004 and 2009, respectively. He is currently an Associate Professor with Hunan University. His research interests include smart grid, load modeling, and electric power automation.

ZHUANGXI TAN was born in Loudi, Hunan, China, in 1991. He received the B.S. degree in electrical engineering from the Hunan Institute of Engineering, Xiangtan, China, in 2013. He is currently pursuing the Ph.D. degree electrical engineering with Hunan University. His research interests include power system control and smart grid.

YANJI ZHOU was born in Xiangtan, Hunan, China, in 1991. He received the B.S. degree in electrical engineering from Xiangtan University, Xiangtan, China, in 2015. He is currently pursuing the M.S. degree with the College of Electrical and Information Engineering, Hunan University, Changsha, China. His major research interests include power system control and smart grid.

CANBING LI (M'06–SM'13) was born in Yiyang, Hunan, China, in 1979. He received the B.S. and Ph.D. degrees in electrical engineering from Tsinghua University, Beijing, China, in 2001 and 2006, respectively. He is currently a Professor with the College of Electrical and Information Engineering, Hunan University, Changsha, China. His research interests include smart grid, energy efficiency, and energy policy.

RUO LI was born in Changde, Hunan, China, in 1993. He received the B.S. degree in electrical engineering from Hunan University, Changsha, China, in 2015, where he is currently pursuing the M.S. degree with the College of Electrical and Information Engineering. His major research interests include power system modeling and simulation.

XUEZHONG QI was born in Shangqiu, Henan, China, in 1991. He received the B.S. degree in electrical engineering from Hunan University, Changsha, China, in 2015, where he is currently pursuing the M.S. degree with the College of Electrical and Information Engineering. His major research interests include power system modeling and simulation.